

Journal of
Mechanics of
Materials and Structures

**VARIATIONAL EIGENSTRAIN ANALYSIS OF
SYNCHROTRON
DIFFRACTION MEASUREMENTS OF RESIDUAL
ELASTIC
STRAIN IN A BENT TITANIUM ALLOY BAR**

Alexander M. Korsunsky

Volume 1, N° 2

February 2006

VARIATIONAL EIGENSTRAIN ANALYSIS OF SYNCHROTRON DIFFRACTION MEASUREMENTS OF RESIDUAL ELASTIC STRAIN IN A BENT TITANIUM ALLOY BAR

ALEXANDER M. KORSUNSKY

Most procedures for experimental stress evaluation rely on the measurement of elastic strain followed by point-wise calculation of stress based on continuum elasticity assumptions despite the fact that the real purpose of the investigation is to characterise the state of stress everywhere in the object to the greatest possible detail. Using the example of residual elastic strain measurements in a bent titanium alloy bar taken by means of high energy synchrotron X-ray diffraction, an interpretation technique is here introduced based on the variational eigenstrain analysis. An analytical framework is presented for the solution of the direct problem of eigenstrain, that is, the calculation of residual elastic strain distribution within an inelastically bent beam containing a known distribution of eigenstrain. An inverse problem about closest matching between the model and experiment is then cast in a form that allows determination of the underlying eigenstrain distribution from a single noniterative solution of a linear system. Subsequently the complete stress state can be reconstructed everywhere within the object in the form of continuous functions. The value of the approach lies in the fact that subsequent deformation modelling can be carried out with the effects of residual stresses (and their evolution) naturally incorporated. The extension of this approach to more complex geometries within the framework of the finite element method is briefly discussed.

1. Introduction

Residual stresses play an important role in determining the deformation behaviour and fatigue durability of engineering components and assemblies. It is well known, for example, that compressive near surface residual stresses act to inhibit crack initiation and propagation, and thus affect the fatigue life of an object. On the other hand, residual stresses themselves are known to undergo modification during thermal and mechanical loading, through various mechanisms related to time-independent plasticity, creep, phase transformation, etc.

We can pursue two principal avenues in evaluating residual stress states: deformation process modelling and experimental measurement.

Keywords: eigenstrain theory, energy-dispersive diffraction, synchrotron, strain mapping.

Numerical simulation of nonlinear deformation behaviour of solid bodies with complex shapes is usually accomplished with the help of the finite element method. This method allows the introduction of sophisticated constitutive laws that take into account kinematic-isotropic nonlinear hardening, cyclic softening or ratcheting, complex creep and stress relaxation behaviour [Manonukul et al. 2005], coupled nonlocal damage and plasticity [Korsunsky et al. 2005], strain gradient effects [Fleck and Hutchinson 2001], etc. Refined models of deformation processes often involve large numbers of material parameters to be determined from experimental measurements. In order to justify the use of process modelling predictions for undertaking practical design decisions, proper validation procedures must be followed.

An alternative approach to residual stress evaluation is via an experimental procedure. In practice, residual stresses are only ever measured indirectly via observing relaxation or their effect on some other physical quantity, for example, bond vibration frequency as in Raman spectroscopy. Experimental techniques for stress evaluation can be classified into relaxation methods, physical correlation methods and diffraction techniques [Withers and Bhadeshia 2001].

Relaxation methods rely on material removal (slitting, hole drilling, blind hole drilling, layer removal, etc.) accompanied by the measurement of either changes in the object shape (monitored by photogrammetry), or changes in strain measured by means of surface mounted strain gauges, as in hole drilling. Physical correlation methods use various physical effects (thermoelastic, magnetoelastic, ultrasound propagation) to obtain some estimate of a stress state parameter—for example, the hydrostatic stress component.

Diffraction is a highly versatile method for direct measurement of interplanar spacing within the atomic lattice. Consequently residual elastic strain can be calculated on the basis of knowledge of strain-free spacing. Diffraction techniques, particularly those using high flux beams generated at synchrotrons [Korsunsky et al. 2002], can be scaled down to allow micro-diffraction and even nano-diffraction experiments. The use of synchrotron X-ray diffraction to provide the input for the current study is described below.

The objective of the present study is to provide a rational solid mechanics basis for the analysis of residual elastic strain data obtained from state-of-the-art synchrotron X-ray diffraction measurements. It must be pointed out, however, that the method described herein possesses great generality, and can be used with equal success to interpret relaxation method data, such as blind hole drilling or slitting techniques. As a vehicle for the introduction of new concepts, a classical problem of residually bent elastic-plastic beam is deliberately chosen for which an analytical solution of the direct eigenstrain problem is available [Korsunsky 2005]. The size

of the bent beam studied was chosen to be commensurate with the size of residually stressed objects routinely studied in the context of power generation and the aerospace industry. The material of the sample was Ti-6Al-4V aerospace titanium alloy used in the manufacture of fan and compressor blades of jet engines.

The article is organised as follows. In [Section 2](#) the theoretical background for the analysis of residual stress states is presented. In [Section 3](#) a concise presentation is given of the background to diffraction techniques for experimental strain analysis. In [Section 4](#) a solution is presented to the ‘direct’ problem of determination of residual elastic strain in a beam from known permanent strain (eigenstrain) distributions. In [Section 5](#) a framework is introduced for variational eigenstrain determination from measured residual elastic strain values, by minimising the sum of squares of model-experiment differences [[Korsunsky et al. 2004](#)]. In [Section 6](#) the results of interpretation of a particular data set are presented and discussed.

2. Theoretical background

Residual stress states in arbitrarily shaped solid bodies are usually complex, and difficult to describe, since in the general case they must be represented by the six components of the stress tensor varying as a function of three spatial variables. It is virtually impossible to imagine an experimental procedure that would readily and routinely provide this level of detail. At any rate, the interpretation of point-wise data in terms of six independent components is likely to present a serious practical challenge.

Any residual stress state described by the tensor σ must, by definition, be self-equilibrating. This requirement in fact establishes a relationship between gradients of different components of the stress tensor, σ , namely

$$\operatorname{div} \sigma = 0. \quad (1)$$

Furthermore, the stress state deduced within a residually stressed object must satisfy the traction-free boundary conditions, namely,

$$\sigma \cdot \mathbf{n} = 0, \quad (2)$$

where \mathbf{n} denotes the surface normal. However, it is not easy to enforce this requirement on the deduced stress state, or to formulate the constraints that must be imposed on the measured strain data. It is possible to develop a rational analytical approach based on the concept of eigenstrain (stored inelastic strain) that reduces the size of the data array needed to represent a particular residual stress state and at the same time guarantees satisfaction of equations of equilibrium, (1), and traction-free boundary conditions (2).

Eigenstrain modelling is a powerful analytical technique for the representation of residual stress states in solids [Mura 1987]. A practical approach to the use of eigenstrain in residual stress modelling can be developed based on the following fundamental postulates [Korsunsky 1997; 2005]:

- (a) In the absence of eigenstrain (stored inelastic strain), any elastic solid is completely free from residual stress. Indeed, the very definition of elastic material response requires that stresses and strains arise in the body upon the application of an external load, and that they vanish completely upon load removal.
- (b) Residual stresses within a solid arise in response to the introduction, through some inelastic mechanism (plasticity, creep, cutting and pasting, phase transformation, etc.), of permanent *nonuniform* strains within the body. Note however that the introduction of an entirely spatially uniform permanent strain field does not, in fact, lead to the generation of residual stresses.
- (c) Elastic and inelastic strains are additive, that is,

$$\boldsymbol{\varepsilon} = \boldsymbol{\varepsilon}^* + \boldsymbol{e}, \quad \text{or in index notation, } \varepsilon_{ij} = \varepsilon_{ij}^* + e_{ij}, \quad (3)$$

where ε_{ij} denotes the total strain, e_{ij} denotes the elastic strain, and ε_{ij}^* denotes eigenstrain.

- (d) Total strain must be compatible, that is, it must satisfy

$$\text{Inc } \boldsymbol{\varepsilon} = \text{rot}((\text{rot } \boldsymbol{\varepsilon})^T) = 0,$$

leading to relationships between strain and components of the type

$$\frac{\partial^2 \varepsilon_{xx}}{\partial y^2} + \frac{\partial^2 \varepsilon_{yy}}{\partial x^2} - \frac{\partial^2 \varepsilon_{xy}}{\partial x \partial y} = 0. \quad (4)$$

- (e) Eigenstrains (permanent inelastic strains) act as the sources of incompatibility of displacement, and so can be thought of as appearing in the right hand of the Saint-Venant compatibility equations. Indeed, from the compatibility equation (4) one readily obtains the ‘incompatibility’ equation for the elastic strain, e_{ij} , in the following form:

$$\frac{\partial^2 e_{xx}}{\partial y^2} + \frac{\partial^2 e_{yy}}{\partial x^2} - \frac{\partial^2 e_{xy}}{\partial x \partial y} = \Xi, \quad (5)$$

where

$$\Xi = \frac{\partial^2 \varepsilon_{xy}^*}{\partial x \partial y} - \frac{\partial^2 \varepsilon_{xx}^*}{\partial y^2} - \frac{\partial^2 \varepsilon_{yy}^*}{\partial x^2}. \quad (6)$$

Note from the above expression that the ‘forcing term’, Ξ , turns to zero for uniform eigenstrains. In fact, it also vanishes for eigenstrains that depend linearly on one coordinate and not at all on other coordinates, so that bodies

containing such residual strain distributions are also free from residual elastic strain, and hence from residual stress.

- (f) The problem of determining the residual elastic fields (residual elastic strain and residual stresses, as well as residual deformations, i.e. distortions) arising from a given eigenstrain, ε_{ij}^* requires the simultaneous solution of equations (5), (1) and (2), together with the elasticity equations (generalised Hooke's law),

$$\sigma = C : e, \quad \text{or in index notation, } \sigma_{ij} = C_{ijkl} \varepsilon_{kl}. \quad (7)$$

- (g) The eigenstrain problem is not in fact in any way different from the well known thermoelastic problem, in which the forcing term Ξ arises from thermal gradients (note that an unconstrained uniformly heated body remains stress-free). In fact, arbitrary eigenstrain distributions can be successfully simulated by means of anisotropic thermal expansion.

Inelastic bending represents one of the most straightforward and well studied processes that leads to the creation of residual stresses. It can be treated very simply within the framework of beam theory whereby only longitudinal elastic strain and stress are considered and differ only by a constant factor that is Young's modulus.

The stresses that arise in inelastic bending can be readily analysed [Gere and Timoshenko 1984] provided the stress-strain behaviour of the sample material under uniaxial tension and compression is known. By modelling numerically the application of a given moment to a beam in bending, the permanent strains induced in the beam by plastic deformation can be readily deduced. Once the externally applied moment is removed, the beam is usually thought to undergo elastic unloading, so the residual stresses and residual elastic strains are easily found.

In the present study a different problem is addressed for which the residual elastic strains after bending are specified in the form of experimental diffraction measurements that may also be subject to some data scatter. The problem is to find the unknown distribution of permanent strains responsible for giving rise to the observed elastic strains. Furthermore, it is also possible to seek to extract approximations to the uniaxial tensile and compressive stress-strain curves from such residual strain data.

3. Experimental

The specimen of Ti64 was machined to the dimensions of $h_y = 50$ mm, $h_x = 8.5$ mm, $h_z = 4$ mm and bent by applying a bending moment M_z of approximately 100 N·m using a 100 kN capacity, screw driven universal testing machine

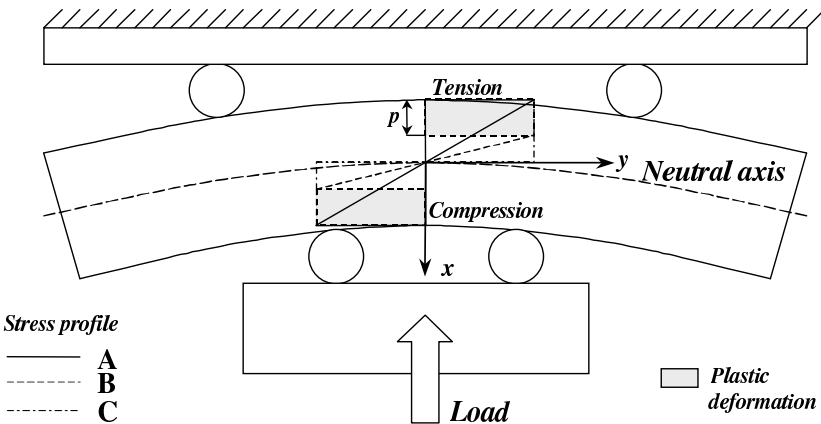


Figure 1. Illustration of plastic deformation of the bar in four point bending.

(Hounsfield Ltd) with a four point bending attachment [Figure 1](#). Under progressively increasing applied bending moment, the lines labelled A, B and C in [Figure 1](#) indicate the profiles of elastic strain, and hence also the longitudinal stress (for the simple case of non-work-hardening material). The elastic strain distribution across the bar remains linear (line A) until the first onset of yielding. Once the applied moment exceeds the yield value (line B), the material undergoes progressive plastic yielding from the surface. Note that the *total* strain remains linear across the beam, but a proportion of it is now accommodated plastically. With the increased applied moment (line C) the tensile and compressive plastic zones expand progressively inwards from two surfaces. In the course of analysis carried out in this paper we pay particular attention to the extent of the plastic zones, the deduction of the distribution of permanent inelastic strains within these zones, and the relationship between these distributions and the macroscopic and microscopic residual stresses.

The two principal methods for extracting residual elastic strain information within objects with the help of X-ray diffraction are the angle-dispersive (monochromatic beam) technique and the energy-dispersive (white-beam) technique.

In obtaining the data used in the present study a single bounce bent Laue mode monochromator was employed [[Laundy et al. 2004](#)] as shown in [Figure 2](#). Bending the Laue monochromator crystal induces tensile and compressive strains on different sides of the crystal, thus increasing the band pass and hence the flux incident on the sample. In many engineering applications this is in fact an advantage, since peak broadening is dominated by sample effects (strain spread within the gauge

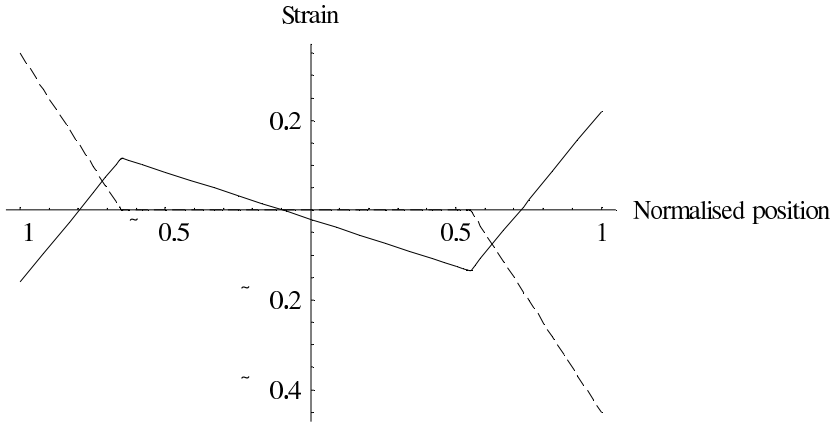


Figure 2. Schematic illustration of the relationship between linear segments of tensile and compressive eigenstrain induced by bending (dashed lines), and the residual elastic strain distribution (solid line) arising by the process of elastic equilibration.

volume), and no advantages are obtained by using extremely fine monochromation.

Diffraction patterns were collected by employing a detector scanning the scattering angle 2θ , or a position sensitive detector capable of registering total photon flux simultaneously at several positions along a line or over a two-dimensional surface. This mode allows accurate determination of diffraction peak intensity, shape and position. However, it usually requires significantly longer counting times in comparison with the white beam mode in order to collect the data from comparable sections of the diffraction pattern, primarily due to the reduction of flux by monochromation, but also due to the necessity of scanning the detector.

Energy dispersive setup allows multiple diffraction peaks to be collected simultaneously, thus achieving particularly efficient counting statistics at energies above 30 keV [Korsunsky et al. 2002]. The accuracy of determination of individual peak position and shape resolution in the white-beam mode is usually related to the resolution of the energy-dispersive detector, but can in fact be several orders of magnitude better. The accuracy of interpretation in terms of lattice parameters and hence strain can be significantly improved by using multiple peak analysis or whole pattern fitting [Liu et al. 2005].

The material used in the present study was a Ti-6Al-4V alloy widely used to manufacture components located at the front of the aeroengine, such as fan and

compressor blades and disks; it also has many other structural applications. Production comprises vacuum arc melting above the β phase transus followed by plate rolling in order to minimise crystallographic texture in the material which results in anisotropy of both elastic and inelastic properties. The structure achieved by the manufacturing process is obtained by solution treating in the middle of the $\alpha + \beta$ phase field and air cooling. This gives a mixture of primary α and a transformation product which comprises α and β phases. The α phase is a hexagonal close-packed structure (hcp) which is typical of titanium at room temperature and transforms to a body centred cubic structure, β phase, at 883°C. The size of the grains was approximately 5 μm .

Bragg's law

$$2d \sin \theta = \lambda = \frac{hc}{E} \quad (8)$$

is used to determine a lattice spacing parameter d that can be related to any particular phase and may correspond to the phase average, if pattern refinement is used, or to the average taken over crystallites of a certain orientation within a particular phase.

The residual elastic strain is computed using the formula

$$e = \frac{d - d_0}{d_0}. \quad (9)$$

For each position of the gauge volume within the sample, peak centre positions were determined for the reflections (00.2), (10.1), (10.2) and (11.0) from the hcp α phase of the titanium alloy, as well as the macroscopic average computed by Pawley refinement of a section of the diffraction profile containing multiple peaks. Unstrained lattice spacing values d_0 for each of these reflections, are also needed to calculate strain using (9). To this end the data were collected by performing a similar measurement for the gauge volume located at the very corner of the sample. This choice of reference was based on the argument that the sampling volume in such a position must be free from tractions (and hence stresses) in the x and y directions. The gauge volume should be free from *macroscopic average* stress, and hence free from macroscopic average residual elastic strain. It should be noted that the above argument does not quite prevent the 'corner' gauge volume from containing microscopic residual stresses that exist between grains of different orientations.

In the sequel an interpretation is developed for the analysis of macroscopic residual elastic strains by employing the eigenstrain formalism. Since this development is undertaken within the framework of continuum elastic theory, the most appropriate residual elastic strain value that should be used for the purpose is that of macroscopic average.

4. Direct problem: determination of residual elastic strain from given eigenstrain

Consider an elastic beam occupying the region $x_L < x < x_R$, $-\infty < y < \infty$ and containing a distribution of eigenstrain $\varepsilon_{yy}^* = \varepsilon^*(x)$. The basic framework for evaluating the residual elastic strain (r.e.s.) distribution that arises in the beam has been presented in [Korsunsky 2005], and will only be reproduced here in brief to introduce some modifications to the previously published results.

The following statements provide the basis for the analysis:

- (i) Total strain in the beam is given by the sum of the elastic and inelastic strain (eigenstrain).
- (ii) Following Kirchhoff's hypothesis of straight normals, it is assumed that material points originally lying on a line perpendicular to the beam axis remain on a straight line, that is, any normal to the beam axis undergoes only rotation without distortion.
- (iii) Hence displacements, and therefore *total* strain must vary linearly through the plate thickness, that is, they must be given by

$$\varepsilon = e + \varepsilon^* = a + bx/h, \quad (10)$$

where $h = x_R - x_L$ is the beam thickness. Here the parameter a characterises the amount of axial straining experienced by the beam, and the term b characterises the intensity of bending.

- (iv) In the absence of external loading being applied, elastic strain e presents an example of macroscopic residual elastic strain, such as that measured in a diffraction experiment.
- (v) From equation (10), residual elastic strain is given by

$$e = a + bx/h - \varepsilon^*(x), \quad (11)$$

If the dependence of parameters a and b on the eigenstrain distribution $\varepsilon^*(x)$ is known, then the relationship between the residual elastic strain e and the eigenstrain is established.

- (vi) It will be shown (below) that parameters a and b depend solely on two integral parameters, namely, the zeroth and first moments of the eigenstrain distribution given by

$$\Gamma = \frac{1}{h} \int_{x_L}^{x_R} \varepsilon^*(x) dx, \quad \Gamma_1 = \frac{1}{h^2} \int_{x_L}^{x_R} \varepsilon^*(x) dx. \quad (12)$$

The relationship between parameters a and b , on the one hand, and Γ and Γ_1 , on the other, is established using the requirements of force and moment balance across

the beam, given by

$$F = \int_{x_L}^{x_R} [a + bx/h - \varepsilon^*(x)] dx = 0, \tag{13}$$

$$M = \int_{x_L}^{x_R} [a + bx/h - \varepsilon^*(x)] x dx = 0. \tag{14}$$

leading to the following relationships:

$$(x_R + x_L) b/2 + a(x_R - x_L) - (x_R - x_L) = 0, \tag{15}$$

$$(x_R^2 + x_R x_L + X_L^2) b/3 + (x_R^2 - x_L^2) a/2 - (x_R - x_L)^2 \Gamma_1 = 0. \tag{16}$$

Expressions are given explicitly in terms of the beam boundaries x_L and x_R for the purposes of generality, e.g., to allow the consideration of effects of surface layer removal.

The solution of the linear system for parameters a and b has the form

$$a = \frac{6\Gamma_1(X_R^2 - x_L^2) - 4\Gamma(x_R^2 + x_L + X_L^2)}{(x_R - x_L)^2}, \tag{17}$$

$$b = \frac{12\Gamma_1(x_R - x_L) - 6\Gamma(x_R - x_L)}{(x_R - x_L)}. \tag{18}$$

Noting that the since bending component of strain in terms of beam bending radius R and the beam curvature K is given by

$$e = \frac{x}{R} = xK, \tag{19}$$

then from equation (8) the curvature of the bent beam is found as

$$K = \frac{b}{h} = \frac{12\Gamma_1(x_R - x_L) - 6\Gamma(x_R - x_L)}{(x_R - x_L)^2}, \tag{20}$$

Equation (20) contains an expression that is useful for the analysis of beam curvature as an function of the eigenstrain distribution $\varepsilon^*(x)$.

Substituting equations (17) and (18) back into equation (11) gives the resulting prediction for the residual elastic strain distribution in the form

$$e(x) = \frac{1}{(x_R - x_L)^2} (6\Gamma_1(x_R - x_L)(2x - x_R - x_L) + 2\Gamma((x_R^2 + x_R x_L + x_L^2) - 3x(x_R + x_L))) - \varepsilon^*(x). \tag{21}$$

Equation (21) establishes the solution of the direct problem about the determination of residual elastic strain for arbitrary given distribution of eigenstrain.

Figure 1 gives an example of the above solution and shows the relationship between the eigenstrain distribution, $\varepsilon^*(x)$, and residual elastic strain e . This result should be seen as the simplest illustration of the relationship between eigenstrain and the residual elastic strain. Although in the present treatment this relationship is established analytically for a rather trivial case, the method is not restricted to such situations. In fact, arbitrary eigenstrain distributions can be readily incorporated into the finite element framework through the use of virtual anisotropic thermal expansion [Korsunsky et al. 2005; Hill 1996].

5. Inverse problem: determination of eigenstrain distribution from measured residual elastic strain

The problem that we wish to address in the present study stands in an inverse relationship to the one solved in the previous section. In practice it is the residual elastic strain distribution that may be known, for example, from diffraction measurement. Alternatively, changes in the elastic strain values can be monitored, say using strain gauges, in the course of material removal; and the underlying eigenstrain distribution then needs to be determined.

In practice the residual elastic strain, or its increments, can only be measured at a finite number of points. We are therefore seeking to *reconstruct* an unknown functional distribution, that is, an object with infinite number of degrees of freedom, using a finite data set. Several difficulties may arise in this situation, e.g. whether the problem described in the previous section can be inverted; whether the inverse problem is regular, i.e. varies in a smooth fashion depending on the data; and whether the obtained solution is unique. In the present study we do not attempt to answer these questions. Instead, we offer an efficient inversion procedure, leaving the evaluation of its uniqueness and regularity for future consideration.

Consider a set of experimental data consisting of the values of residual elastic strain (r.e.s.) y_j collected at positions x_j , $j = 1, \dots, m$. In the present study we assume that the data was collected from a one-dimensional scan in coordinate x . It is worth noting, however, that the approach presented below is not in any way limited to one-dimensional problems, and can be readily generalised to two- and three-dimensional cases.

Denote by $e(x)$, as in the previous section, the *predicted*, or *modelled* residual elastic strain distribution. Evaluating $e(x)$ at each of the measurement points gives the *predicted values* $e_j = e(x_j)$. In order to measure the goodness of the prediction we form a functional J given by the sum of squares of differences between actual

measurements and the predicted values, with weights:

$$J = \sum_{j=1}^m w_j (y_j - e_j)^2. \quad (22)$$

The choice of weights w_j is left to the modeller; for example, they could be chosen based on the accuracy of measurements being interpreted.

Minimisation of functional J provides a rational variational basis for selecting the most suitable model to match the measurements, in terms of the overall goodness of fit.

Let us now assume that the unknown eigenstrain distribution, yet to be determined, is given by a truncated series of *basis* distributions,

$$e^*(x) = \sum_{i=1}^N c_i \xi_i(x). \quad (23)$$

Here N is the total number of *basis* distributions used in the prediction.

The results of the previous section contain the analytical procedure for the solution of the direct problem, that is, the determination of the residual elastic strain distribution that arises in response to an arbitrary eigenstrain distribution $e^*(x)$. This procedure can now be applied to each of the N basis distributions $\xi_i(x)$ in turn. As a result, a family of residual elastic strain solutions $E_i(x)$ is obtained.

Due to the linearity of the direct problem, the predicted values of e_j the residual elastic strain arising from the eigenstrain distribution $\varepsilon^*(x)$ of equation (23) can themselves be written in the form of a superposition of responses to the *basis* eigenstrain distributions,

$$e_j = \sum_{i=1}^N c_i E_i(x_j) = \sum_{i=1}^N c_i e_{ij}, \quad (24)$$

with the same coefficients c_i as in equation (23).

The inverse problem of determining the unknown eigenstrain distribution $\varepsilon^*(x)$ has now been reduced to the problem of determination of N unknown coefficients c_i that deliver a minimum to the functional J in equation (22), which may now be rewritten as

$$J = \sum_{j=1}^m w_j \left(\sum_{i=1}^N c_i e_{ij} - y_j \right)^2. \quad (25)$$

The above expression is quadratic and positive definite in the unknown coefficients c_i . It follows that the functional has a unique minimum that is found by

satisfying the condition

$$\nabla_c J = 0, \quad \text{or} \quad \frac{\partial J}{\partial c_i} = 0, \quad i = 1, \dots, N. \quad (26)$$

Due to the quadratic nature of the functional in equation (25), the system of equations in equation (26) is linear. Therefore, the solution for the unknown coefficients c_i can be readily found *without iteration* by inverting the linear system arising in equation (26). This system is written out explicitly below.

The partial derivative of J with respect to the coefficient c_i can be written explicitly as

$$\frac{\partial J}{\partial c_i} = 2 \sum_{j=1}^m w_j e_{ij} \left(\sum_{k=1}^N c_k e_{kj} - y_j \right) = 2 \left(\sum_{k=1}^N c_k \sum_{j=1}^m w_j e_{ij} e_{kj} - \sum_{j=1}^m w_j e_{ij} y_j \right) = 0. \quad (27)$$

For purposes of illustration, let us now assume that the weights are equal to unity, so that equation (27) simplifies to:

$$\frac{\partial J}{\partial c_i} = 2 \left(\sum_{k=1}^N c_k \sum_{j=1}^m e_{ij} e_{kj} - \sum_{j=1}^m e_{ij} y_j \right) = 0. \quad (28)$$

We introduce the following matrix and vector notation

$$\mathbf{E} = \{e_{ij}\}, \quad \mathbf{y} = \{y_j\}, \quad \mathbf{c} = \{c_i\}. \quad (29)$$

Noting that notation e_{kj} corresponds to the transpose of matrix E , the entities appearing in (28) can be written in matrix form as:

$$\mathbf{A} = \sum_{j=1}^m e_{ij} e_{kj} = \mathbf{E}\mathbf{E}^T, \quad \mathbf{b} = \sum_{j=1}^m e_{ij} y_j = \mathbf{E}\mathbf{y}. \quad (30)$$

Hence equation (28) assumes the form

$$\nabla_c J = 2(\mathbf{A}\mathbf{c} - \mathbf{b}) = 0. \quad (31)$$

The solution of the inverse problem has thus been reduced to the solution of the linear system

$$\mathbf{A}\mathbf{c} = \mathbf{b} \quad (32)$$

for the unknown vector of coefficients $\mathbf{c} = \{c_i\}$.

Whenever the solution of an inverse problem is sought, questions arise concerning the existence and uniqueness of the solution, and also concerning the well-posedness of the problem, that is, the continuity of the dependence of the solution on the problem parameters, the choice of the basis functions, the number of terms N in the truncated series, etc.

Within the present regularised formulation of the problem, for an *arbitrary* choice of the family of basis functions and an *arbitrary* number of basis functions N , a unique solution is guaranteed to exist. This is a consequence of the positive definiteness of the quadratic functional J . Furthermore, it is clear that increasing the number of terms N is guaranteed to deliver a sequence of monotonically non-increasing values of J , in other words, the goodness of approximation will not be diminished.

An interesting question concerns the convergence of the solution in terms of eigenstrain distribution $\varepsilon^*(x)$, to the ‘true’ solution in the limit $N \rightarrow \infty$. Similarly, the continuity in the behaviour of the solution with the choice of basis functions deserves to be discussed. While it must be emphasised that these questions are clearly fundamental and ought to be addressed, the focus is currently placed on the development of a practical tool for residual strain analysis. In so far as this is the aim of the present study, the proposed framework offers an efficient ‘one shot’ approach to the solution of an inverse problem. Furthermore, the choice of moderate values N , compared to the number of measurements, m , also offers a rational procedure for smoothing the data.

Figure 2 illustrates the relationship between the simple kind of eigenstrain distribution that may be introduced by inelastic bending (shown by the dashed lines) in tension and compression on the opposites sides of the sample, and the residual elastic strain (shown by the solid line) that arises by the process of elastic equilibration in response. For simplicity, the eigenstrain distributions are assumed to be linear in both tension and compression. This assumption corresponds to the case of elastic-ideally plastic material. Note, however, that the depths of the plastic zones on the two sides of the sample are allowed to be different. As a result the residual elastic strain state that arises in the bent beam is asymmetric, and illustrates how asymmetry of residual stress distribution is connected with the asymmetry of material response (yielding) in tension and compression.

6. Results and discussion

The variation procedures for eigenstrain determination described in the previous section were applied to the experimental data obtained from synchrotron diffraction measurements. As noted earlier, the diffraction strain estimate that is obtained by whole pattern refinement provides the most reliable estimate of the average macroscopic residual elastic strain. These data were used in the present analysis.

The unknown eigenstrain distributions were represented by the following series:

$$\varepsilon^{*T} = \sum_{i=1}^N c_i(x-d)^i, \quad \varepsilon^{*C}(x) = - \sum_{i=1}^N c'_i(x-d')^i, \quad (33)$$

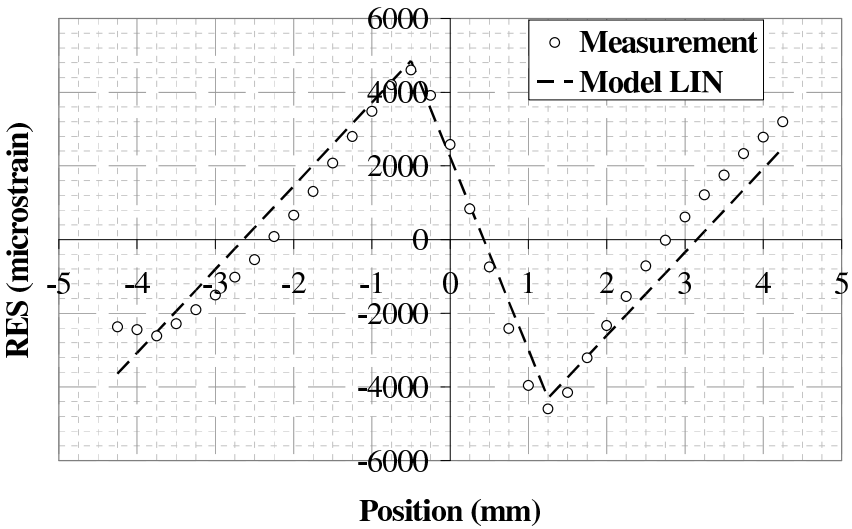


Figure 3. The measured profile of residual elastic strains in the bent Ti-6Al-4V bar (markers) compared with the prediction of the linear eigenstrain model (dashed line).

where superscripts refer to the tensile and compressive eigenstrains, and parameters d and d' denote the positions of the tensile and compressive plastic zone boundaries, respectively.

Several versions of the variational interpretation were investigated. In the first version a very simple interpretation was used of the type illustrated in Figure 2, that is, with linear assumed eigenstrain profiles in both tension and compression. Nevertheless, even with such simple assumptions it was possible to capture the salient features of the residual elastic strain distribution. The comparison between the model and experiment is illustrated in Figure 3, where the experimental measurement points are shown by the markers, while the continuous line shows the model prediction obtained using only the linear terms in the eigenstrain distribution. Note that the eigenstrain interpretation provides a ‘balanced’ approximation in the least squares sense; the model provides a ‘smoothing’ of the data at the chosen level of detail in the description of eigenstrain distribution.

Figure 4 shows the improvement to the model prediction afforded by allowing higher order of eigenstrain distribution functions (up to order 6): the agreement between the model and experimental measurements shown by markers is clearly improved. However, in the model used for this reconstruction the tensile and compressive eigenstrain distributions remained linked, in that the same coefficients were used in the expressions for the tensile and compressive eigenstrains in equation (33), that is, $c'_i = c_i$.

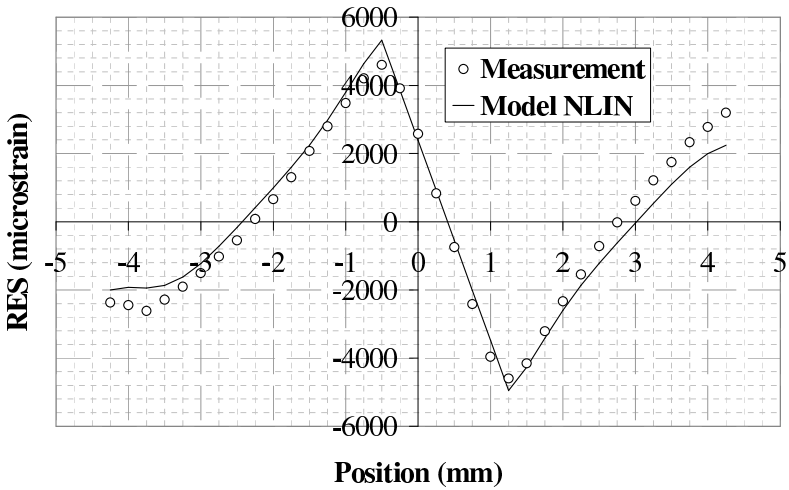


Figure 4. The measured profile of residual elastic strains in the bent Ti-6Al-4V bar (markers) compared with the predictions of the higher order eigenstrain model (continuous curve).

Figure 5 shows the result of interpretation, with the coefficients for the tensile and compressive eigenstrain distributions allowed to vary independently, that is, $c'_i \neq c_i$. Some small improvement can be detected, although it is not thought to be particularly significant.

Finally, in Figure 6 the order of approximation was increased to $N = 10$. This clearly delivers an improvement in the apparent quality of fit, but also leads to some oscillatory behaviour of the prediction curve. This situation might perhaps be expected for any approximation that involves higher order polynomial representation of an unknown distribution. The problem of this type could be overcome by representing the unknown distribution by a set of smooth radial basis functions with bounded support.

7. Conclusions

The purpose of the present paper was to introduce a self-contained framework that can serve as a convenient vehicle for introducing the fundamental ideas for residual stress reconstruction using the concept of continuous distributions of eigenstrain. Kirchhoff bending theory allows a simple analytical formulation to be developed for the prediction of the residual elastic strain (and hence bending stress) within inelastically bent bars due to distributions of tensile and compressive eigenstrains.

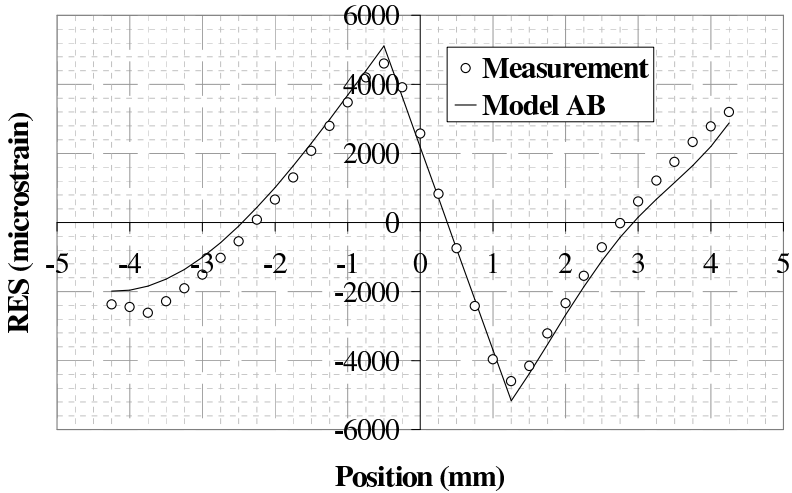


Figure 5. The measured profile of residual elastic strains in the bent Ti-6Al-4V bar (markers) compared with the predictions of the higher order eigenstrain model (continuous curve) with separate description of the tensile and compressive eigenstrain distributions.

Once these analytical formulae are established, they are used as the direct eigenstrain problem solver within the inverse framework for variational determination of unknown eigenstrains.

The solutions are obtained for residual elastic strain profiles measured by high energy synchrotron X-ray diffraction. The stability of the solutions is investigated by way of numerical experiments involving different formulation of the functional basis and different orders of approximation. It is found that the solutions display good stability, although the use of higher order polynomial approximations leads to some evidence of oscillatory behaviour of the solution. An approach using radial basis functions may be able to overcome this difficulty.

The findings of this paper are particularly relevant to the task of modelling the effects of residual stresses on subsequent deformation behaviour of engineering components. Assuming the residual elastic strain distribution can somehow be measured, for example, by diffraction, the underlying eigenstrain distribution can then be determined via an implementation of the variational approach presented here. When once such distribution is found, it can be used to continue deformation simulation onwards from the corresponding instant in the component's history. It then becomes possible not only to account accurately for the effects of residual

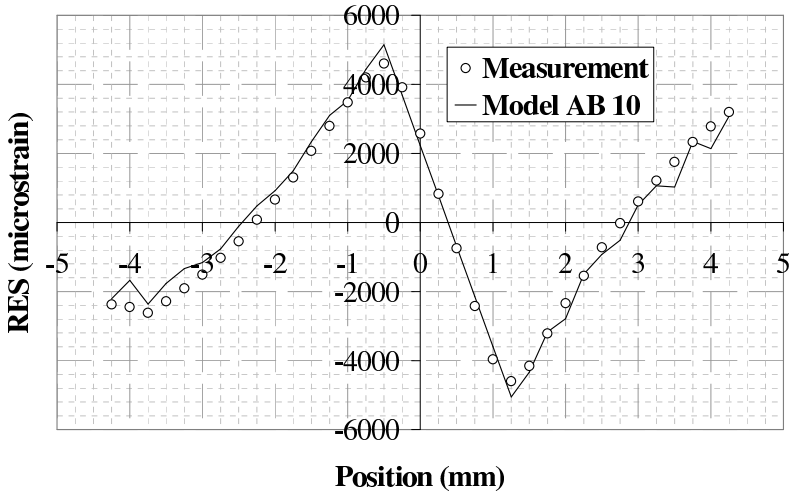


Figure 6. The measured profile of residual elastic strains in the bent Ti-6Al-4V bar (markers) compared with the predictions of the higher order eigenstrain model (continuous curve) with high order ($N = 10$) separate description of the tensile and compressive eigenstrain distributions.

stresses on subsequent deformation, but also *vice versa* to observe the evolution of the residual stress state (or, perhaps even more appropriately, of the underlying eigenstrain distribution) under deformation.

References

- [Fleck and Hutchinson 2001] N. A. Fleck and J. W. Hutchinson, “A reformulation of strain gradient plasticity”, *J. Mech. Phys. Solids* **49** (2001), 2245–2271.
- [Gere and Timoshenko 1984] J. M. Gere and S. P. Timoshenko, *Mechanics of materials*, Chapman and Hall, London, 1984.
- [Hill 1996] M. R. Hill, *Determination of residual stress based on the estimation of eigenstrain*, Ph.D. Thesis, Stanford University, 1996.
- [Korsunsky 1997] A. M. Korsunsky, “An analysis of residual stresses and strains in shot peening”, in *5th Intl. Conf. Residual Stresses*, edited by T. Ericsson, Linköping, Sweden, 1997.
- [Korsunsky 2005] A. Korsunsky, “On the modelling of residual stresses due to surface peening using eigenstrain distributions”, *J. Strain Anal.* **40** (2005), 817–824.
- [Korsunsky et al. 2002] A. M. Korsunsky, S. P. Collins, R. A. Owen, M. R. Daymond, S. Achtioui, and K. James, “Fast residual stress mapping using energy-dispersive synchrotron X-ray diffraction on station 16.3 at the SR S”, *J. Synch. Rad.* **9** (2002), 77–81.

- [Korsunsky et al. 2004] A. M. Korsunsky, K. E. James, and M. R. Daymond, “Intergranular stresses in polycrystalline fatigue: diffraction measurement and self-consistent modelling”, *Eng. Fract. Mech.* **71** (2004), 805–812.
- [Korsunsky et al. 2005] A. M. Korsunsky, G. D. Nguyen, and G. T. Houlsby, “Analysis of essential work of rupture using non-local damage-plasticity modelling”, *Intl. J. Fract.* **135** (2005), L19–26.
- [Laundy et al. 2004] D. Laundy, A. Lennie, M. Golshan, D. Taylor, M. Roberts, G. Bushnell-Wye, R. Cernik, J. Flaherty, and I. Burrows, “A focusing Laue monochromator optimised for diamond anvil cell diffraction experiments”, pp. 683–686 in *Synchrotron radiation instrumentation*, vol. 705, San Francisco, 2004.
- [Liu et al. 2005] J. Liu, K. Kim, M. Golshan, D. Laundy, and A. M. Korsunsky, “Energy calibration and full-pattern refinement for strain analysis using energy-dispersive and monochromatic x-ray diffraction”, *J. Appl. Cryst.* **38** (2005), 661–667.
- [Manonukul et al. 2005] A. Manonukul, F. P. E. Dunne, D. Knowles, and S. Williams, “Multiaxial creep and cyclic plasticity in nickel-base superalloy C263”, *Intl. J. Plasticity* **21** (2005), 1–20.
- [Mura 1987] T. Mura, *Micromechanics of defects in solids*, Nijhoff, Dordrecht, 1987.
- [Withers and Bhadeshia 2001] P. J. Withers and H. K. D. H. Bhadeshia, “Residual stress, I: Measurement techniques”, *Mats. Sci. Technol.* **17** (2001), 355–365.

Received 10 Oct 2005.

ALEXANDER M. KORSUNSKY: *Department of Engineering Science, University of Oxford, Parks Road, Oxford OX1 3PJ, UK*

alexander.korsunsky@eng.ox.ac.uk

<http://www.eng.ox.ac.uk/~ftgamk>